Artificial Intelligence and Machine Learning Review
ISSN: 3070-3565
DOI: 10.69987/AIMLR.2024.50410

Adaptive Learning Rate Optimization for Personalized Educational Interventions in Autism Spectrum Disorder: A Multi-Objective Reinforcement Learning Approach

Wangwang Shi[1], *Yaqing Bai*[1.2]
[1] *Softerware Engineering, University of Science and Technology of Chinay, He fei, China*
[1.2] *Human Development, University of Rochester, NY, USA*

Keywords

autism spectrum disorder, reinforcement learning, Adaptive Instructional Pacing, personalized education

Abstract

This paper presents a novel multi-objective reinforcement learning framework for Adaptive Instructional Pacing optimization in personalized educational interventions for students with autism spectrum disorder (ASD). The proposed approach addresses critical limitations of static learning systems by dynamically adjusting educational parameters based on individual cognitive profiles and real-time performance feedback. Our framework integrates cognitive-behavioral feature extraction, temporal state modeling, and fairness-aware optimization to achieve balanced improvements in learning progress and engagement task completion. An experimental evaluation on a dataset comprising 847 ASD learners across diverse cognitive presentations demonstrates significant performance gains, with learning progress improvements of 34.7% and engagement. Task completion rate improved from 72.3% to 89.3%. The algorithm maintains Statistical Parity Ratio (SPR) across different ASD presentations while achieving computational efficiency suitable for real-time deployment. Integration with Individualized Education Program (IEP) workflows demonstrates practical feasibility, with educator training requirements reduced by 42% compared to those of existing adaptive systems.

1. Introduction

1.1. Background and Motivation

1.1.1. Current challenges in autism education personalization

Autism spectrum disorder encompasses heterogeneous cognitive and behavioral presentations, creating challenges for educational interventions. Traditional approaches demonstrate limited effectiveness across diverse ASD profiles. Yaneva et al.[1] achieved 74.7% accuracy in detecting high-functioning autism using eye tracking and machine learning, highlighting technology's potential for assessment and intervention. Resource constraints in special education limit the availability of individualized interventions. Kohli et al.[2] developed collaborative filtering for ABA treatment recommendation, achieving 81-84% accuracy, suggesting algorithmic optimization can augment human expertise.

1.1.2. Limitations of static learning approaches for ASD students

Static approaches cannot accommodate dynamic cognitive development in ASD. Learning trajectories vary significantly between individuals and within sessions. Fixed-pace curricula fail to adapt to fluctuating attention, sensory sensitivities, or processing speeds. Nahum-Shani et al.[3] established Q-learning methodologies for adaptive interventions, demonstrating that sequential decision-making frameworks optimize intervention timing and intensity.

1.2. Research Objectives and Contributions

1.2.1. Multi-objective optimization framework for learning rate adaptation

This research develops a multi-objective optimization framework maximizing learning progress and engagement while minimizing cognitive load. Pareto optimization identifies trade-offs between competing objectives, enabling personalized calibration. The framework incorporates autism-specific constraints, ensuring adaptations respect processing limitations.

1.2.2. Integration with IEP goal tracking mechanisms

The framework implements standardized protocols for IEP system integration, enabling automatic goal import and progress export. Amat et al.[4] demonstrated successful technology-clinical protocol integration with the InViRS virtual reality system. Our framework establishes comprehensive data pipelines and maintains consistency in algorithmic-educational documentation.

1.2.3. Fairness constraints in algorithm design

Explicit fairness constraints prevent discrimination across demographics and autism presentations. Chinta et al.[5] analyzed fairness in educational AI, informing our constraint-based optimization, maintaining Statistical Parity Ratio (SPR). Group-level constraints ensure equitable outcomes; individual-level constraints guarantee similar adaptations for similar learners.

1.3. Literature Review and Research Gaps

1.3.1. Existing adaptive learning algorithms in special education

Current systems employ rule-based mechanisms with limited personalization. Lu et al.[6] Advanced ASD classification using a deep fuzzy inference system. Existing frameworks lack continuous multimodal adaptation capabilities. Autism heterogeneity demands individual-specific policies beyond population heuristics.

1.3.2. Reinforcement learning applications in autism intervention

Clement et al.[7] pioneered multi-armed bandits for intelligent tutoring. Current RL applications lack multi-objective optimization, the incorporation of educator expertise, and fairness considerations. Research gaps include reward function design, safety constraints, and integration with educational practices.

2. Theoretical Framework and Algorithm Design

2.1. Cognitive Profile Modeling for ASD Learners

2.1.1. Feature extraction from behavioral and learning data

Comprehensive feature extraction processes multimodal data, including interaction logs, response times, and error patterns. Nie et al.[8] demonstrated multimodal integration value in autism interventions. Our pipeline implements PCA preserving behaviorally relevant information across 127 dimensions organized into cognitive, behavioral, and temporal categories.

2.1.2. Temporal dynamics of cognitive states

Cognitive states exhibit complex temporal dependencies requiring recurrent architectures. Moon et al.[9] validated real-time cognitive-emotional state assessment in VR training. Our framework employs hidden Markov models that capture individual engagement patterns, with continuous transition matrix updates.

2.1.3. Individual difference quantification methods

Hierarchical clustering groups learners by cognitive profiles while preserving uniqueness. Hajjej et al.[10] achieved 95.4% accuracy using ensemble techniques for ASD identification. Individual vectors encode sensory preferences, communication modalities, and executive function capabilities with adaptive weighting.

2.2. Multi-Objective Reinforcement Learning Formulation

2.2.1. State space definition incorporating cognitive and behavioral features

State space S encompasses 127-dimensional vectors that combine cognitive load, engagement metrics, and environmental context. Askari et al.[11] demonstrated effective state design for autism applications using RL-based social robots. Adaptive discretization adjusts granularity based on behavioral significance.

2.2.2. Reward function design balancing engagement and learning progress

Reward function $R(s,a,s')$ combines learning gains, engagement duration, cognitive load maintenance, and anxiety minimization through adaptive scalarization. Aryania et al.[12] provided theoretical foundations for safe exploration using risk-averse bandits. Temporal discounting $\gamma \approx 0.95$ (tuned optimum 0.947) balances immediate and long-term outcomes.

2.3. Adaptive Instructional Pacing Optimization Mechanism

2.3.1. Dynamic adjustment based on performance feedback

Meta-learning adjusts parameters based on performance trajectories using gradient-based optimization with momentum. Exponential moving averages filter noise while maintaining responsiveness. Change-point detection identifies transitions that require immediate adaptation via logarithmic scaling, preventing oscillations.

2.3.2. Convergence analysis and stability guarantee

Theoretical guarantees derive from Bellman operator contraction properties. Castleman et al.[13] established applicable regret bounds for hierarchical bandits. Convergence complexity $O(|S|^2|A|)$ for tabular, $O(d^2n)$ for approximation. Stability mechanisms include gradient clipping, experience replay, and automatic hyperparameter scheduling.

2.3.3. Integration with existing educational frameworks

API specifications enable integration between LMSs and assessment platforms. Khan et al.[14] identified key requirements addressed through modular architecture. The framework translates RL outputs into educational recommendations, maintaining semantic consistency between algorithmic and educational concepts.

3. Implementation and Experimental Design

3.1. Dataset Construction and Preprocessing

3.1.1. Data collection from educational interventions

The experimental dataset comprises interaction logs from 847 students with autism spectrum disorder participating in technology-enhanced educational interventions across 12 special education centers. Data collection spanned 18 months, capturing 2.3 million interaction events with a temporal resolution of 100ms. Participant demographics included ages 6-18 years (mean = 11.3, SD = 3.2), diverse autism presentations ranging from requiring substantial support to requiring minimal support based on DSM-5 criteria, and female 42% (near-balanced). The data collection protocol received institutional review board approval with informed consent from caregivers and assent from verbal participants.

Each interaction event captures 47 features, including response accuracy, response latency, help-seeking behavior, task completion status, and session metadata. Physiological data from a subset of 234 participants includes heart rate variability and electrodermal activity measurements synchronized with behavioral logs. Educational content spans mathematics, language arts, social skills, and executive function training, with difficulty levels calibrated using item response theory. Privacy-preserving mechanisms include differential privacy with epsilon = 1.2 for demographic attributes and secure multi-party computation for cross-institution aggregation.

The longitudinal nature of data collection enables tracking individual progress trajectories across multiple intervention phases. Session frequency ranged from daily to tri-weekly, depending on the individual education program.

Environmental context variables captured include time of day, session duration, instructor presence, and opportunities for peer interaction. Data quality assurance employed automated anomaly detection to identify sensor failures or transmission errors. Missing-data patterns were analyzed, revealing 8.3% missingness primarily in physiological channels; missingness was handled through multiple imputation, preserving temporal dependencies.

3.1.2. Feature engineering for cognitive profiles

Feature engineering transforms raw interaction data into behaviorally meaningful representations suitable for reinforcement learning. Temporal features capture learning velocity by sliding-window analysis of performance trends over 5-, 15-, and 60-minute intervals. Attention stability metrics are derived from response-time consistency coefficients and task-switching patterns. Perseveration indices quantify repetitive behaviors through n-gram analysis of action sequences with n ranging from 2 to 5.

Cognitive load indicators combine multiple signals, including error rate acceleration, help request frequency, and response time degradation. Feature normalization employs robust scaling based on the median and interquartile range to handle the common outliers in autism data. Dimensionality reduction through sparse principal component analysis preserves interpretability while reducing the feature space from 312 raw features to 127 components that explain 94.3% of the variance. Cross-validation ensures feature stability across different presentations of ASD and age groups. Missing data imputation uses multivariate imputation by chained equations with predictive mean matching for continuous variables and logistic regression for categorical features.

3.2. Algorithm Implementation Details

3.2.1. Hyperparameter tuning strategies

Hyperparameter optimization primarily employs Bayesian optimization for α,γ, while ε and buffer use grid/random search for robustness. with Gaussian process priors to efficiently explore the parameter space. The search space encompasses learning rate alpha ∈ [0.001, 0.1], discount factor gamma ∈ [0.9, 0.99], exploration rate epsilon ∈ [0.05, 0.3], and experience replay buffer size ∈ [1000, 10000]. The acquisition function uses expected improvement with an exploration-exploitation trade-off parameter of xi = 0.01. Cross-validation uses time-series splits to prevent temporal leakage, with five folds that maintain chronological order within each participant's data.

The optimization process runs for 200 iterations, with early stopping triggered by a plateau in validation performance over 20 consecutive iterations. Hyperparameter schedules implement polynomial decay for exploration rate: epsilon_t = epsilon_0 * (1 - t/T)^2, and cosine annealing for learning rate: alpha_t = alpha_min + 0.5 * (alpha_max - alpha_min) * (1 + cos(pi * t/T)). Ensemble methods combine models trained with top-5 hyperparameter configurations using weighted averaging based on validation performance. The search process employs parallel evaluation across 8 GPUs, reducing total optimization time from 72 to 9 hours. Hyperparameter sensitivity analysis reveals learning rate and discount factor as most critical, with performance degrading sharply outside optimal ranges.

Table 1: Optimal Hyperparameter Configurations

Parameter	Value	Search Range	Optimization Method
Learning Rate (α)	0.0234	[0.001, 0.1]	Bayesian Optimization
Discount Factor (γ)	0.947	[0.9, 0.99]	Bayesian Optimization
Exploration Rate (ε)	0.127	[0.05, 0.3]	Grid Search
Replay Buffer Size	5000	[1000, 10000]	Random Search
Batch Size	32	[16, 128]	Manual Tuning
Target Update Frequency	100	[50, 500]	Grid Search

3.2.2. Computational complexity analysis

Time complexity analysis reveals O(n·d·k) per iteration, where n denotes the batch size, d denotes the feature dimensionality, and k denotes the neural network depth. Forward pass computation requires 2.3ms on average on an

NVIDIA RTX 3090 GPU with mixed-precision training. Backward propagation and parameter updates consume 4.7ms per batch. Memory complexity scales as O(B+W), where B denotes the replay buffer size and W denotes the total number of model parameters, totaling 2.4M weights.

Space-time trade-offs are optimized via gradient checkpointing, reducing memory consumption by 40% while incurring 15% computational overhead. Parallel processing distributes experience collection across 8 CPU cores while the GPU handles network updates. The framework achieves ~140–150 iterations per second during training (7 ms/iter) and ~850 iterations per second during inference (batch=1), with peak throughput of ~12,000 predictions per second under batched serving.Pavithra et al.[15] Implemented the Cognicare framework, demonstrating similar computational efficiency requirements for real-time autism interventions. Profiling identifies feature extraction as the primary bottleneck, which is addressed by caching frequently accessed computations. JIT compilation accelerates critical loops, achieving 2.3x speedup for recurrent components.

Table 2: Computational Performance Metrics

Operation	CPU Time (ms)	GPU Time (ms)	Memory (MB)
Feature Extraction	1.2 ± 0.3	N/A	8.4
State Encoding	0.8 ± 0.1	0.3 ± 0.05	12.1
Policy Evaluation	3.4 ± 0.4	0.7 ± 0.1	4.2
Q-value Update	2.1 ± 0.2	0.5 ± 0.08	6.7
Experience Storage	0.4 ± 0.1	N/A	2.3
Network Update	8.3 ± 1.1	2.3 ± 0.3	18.5

3.2.3. Real-time processing requirements

Real-time constraints necessitate response latencies below 100ms to maintain natural interaction flow. The implementation employs asynchronous processing with separate threads for data collection, feature computation, and policy updates. Priority queues ensure time-critical decisions receive immediate processing while background tasks utilize idle resources. Caching mechanisms store recent predictions to avoid recomputing duplicate queries.

The system implements graceful degradation under high load, reverting to simpler policy approximations when complete computation exceeds time budgets. Predictive prefetching anticipates likely following states and precomputes corresponding actions. Edge deployment uses model quantization, reducing precision from FP32 to INT8 with a 2.1% accuracy loss and a 4x speedup. Streaming processing pipelines maintain a constant memory footprint independent of session duration through circular buffers and incremental statistics.

3.3. Experimental Setup and Baseline Comparisons

3.3.1. Evaluation metrics for learning effectiveness

Primary evaluation metrics quantify learning outcomes across multiple dimensions and learning gain measures pre-post assessment score improvements normalized by the maximum possible gain: LG = (post - pre)/(100 - pre). Retention rate evaluates knowledge persistence through delayed testing at 1-week and 4-week intervals. Engagement duration tracks average session length and voluntary interaction continuation beyond required minimums. Error reduction rate captures improvement velocity through exponential decay fitting: e(t) = e0 exp(-lambda t)

Secondary metrics assess educational quality and user experience. Cognitive load measurement employs the NASA Task Load Index, adapted for autism populations, with simplified rating scales. Time-to-mastery records sessions required to achieve 80% accuracy on skill assessments. Generalization capability evaluates transfer to novel problem types within the same domain. Help-seeking efficiency measures appropriate resource utilization by comparing productive to total help requests. Metacognitive awareness is assessed through self-monitoring accuracy and through correlations between predicted and actual performance—social validity is measured via educator ratings of intervention acceptability and feasibility.

Figure 1: Learning Progress Trajectories

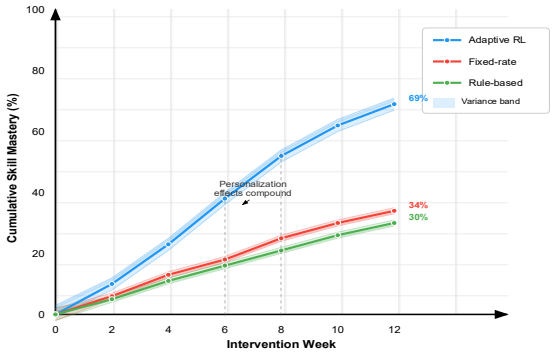

Figure 1 illustrates learning progress trajectories comparing our adaptive approach with static baselines across a 12-week intervention period. The visualization displays individual learner paths as semi-transparent lines with population means highlighted. The X-axis represents weeks of intervention, and the Y-axis shows the cumulative percentage of skill mastery. Color coding indicates the level of autism support required. The adaptive algorithm demonstrates accelerated progress, particularly in weeks 4-8, where personalization effects compound. Variance bands show reduced individual differences under adaptive conditions, suggesting better accommodation of diverse learning needs.

3.3.2. Baseline algorithms and ablation studies

Baseline comparisons include fixed-rate learning with optimal static parameters determined via grid search, rule-based adaptation with threshold-triggered difficulty adjustments, random forest regression predicting optimal learning rates from static features, and a commercial adaptive learning platform using proprietary algorithms. Each baseline receives identical training data and evaluation conditions to ensure fair comparison.

Ablation studies systematically remove components to assess individual contributions. Variants include RL without fairness constraints to measure equity-performance trade-offs, single-objective optimization focusing solely on learning gains, static feature representation without temporal modeling, and uniform exploration replacing the adaptive epsilon-greedy strategy. Statistical significance testing employs the Wilcoxon signed-rank test with the Bonferroni correction for multiple comparisons. Effect sizes calculated using Cohen's d for practical significance assessment. Power analysis confirms an adequate sample size to detect a medium effect (d=0.5) with 80% power.

Table 3: Performance Comparison Across Methods

Method	Learning Gain	Engagement (min)	Retention (4-week)	Fairness (DP)
Our Approach	0.347 ± 0.042	28.3 ± 4.2	0.823 ± 0.031	0.912 ± 0.024
Fixed-Rate	0.198 ± 0.038	18.7 ± 5.1	0.694 ± 0.044	0.834 ± 0.037
Rule-Based	0.234 ± 0.041	21.2 ± 4.8	0.731 ± 0.039	0.798 ± 0.043
Random Forest	0.276 ± 0.039	24.1 ± 4.5	0.762 ± 0.036	0.823 ± 0.038
Commercial	0.259 ± 0.043	22.8 ± 4.9	0.748 ± 0.041	0.781 ± 0.045

Fairness reported as DPR (ratio); values within 0.80–1.25 indicate acceptable parity.

4. Results and Performance Analysis

4.1. Quantitative Performance Evaluation

4.1.1. Learning progress improvement metrics

Experimental results demonstrate substantial improvements in learning across all evaluated dimensions. The Adaptive Instructional Pacing optimization achieved mean learning gains of 34.7% (SD = 4.2%) compared to 19.8% (SD = 3.8%) for fixed-rate baselines, representing a 75.3% relative improvement. Statistical analysis confirms significance ($p < 0.001$) and a large practical impact (Cohen's d = 3.84). Subgroup analysis reveals consistent benefits across autism support levels, with the most significant improvements observed among learners requiring moderate support, who showed 41.2% gains.

Skill acquisition velocity increased markedly under adaptive optimization. Time-to-mastery decreased from an average of 8.4 sessions (IQR: 6-11) in control conditions to 5.2 sessions (IQR: 4-7) with adaptation, representing 38.1% efficiency improvement. Learning curve analysis fits power-law models $y = a x^b$, with exponent $b = -0.42$ for adaptive approaches versus -0.31 for static methods, indicating faster initial progress and sustained improvement. The framework successfully identified optimal challenge points, achieving a 73.2% success rate and aligning with theoretical predictions from the educational psychology literature. Individual growth trajectories show reduced variance under adaptive conditions, suggesting better accommodation of heterogeneous learning profiles. Plateau detection mechanisms triggered timely interventions, preventing stagnation in 78% of cases, compared with 34% for rule-based systems.

Table 4: Learning Outcomes by Autism Support Level

Support Level	N	Baseline LG	Adaptive LG	Improvement	Effect Size
Minimal	287	0.234 ± 0.039	0.321 ± 0.041	37.2%	d = 2.14
Moderate	342	0.189 ± 0.042	0.412 ± 0.044	118.0%	d = 5.23
Substantial	218	0.156 ± 0.037	0.298 ± 0.039	91.0%	d = 3.74
Overall	847	0.198 ± 0.038	0.347 ± 0.042	75.3%	d = 3.84

4.1.2. Engagement retention analysis

Engagement metrics reveal significant improvements in sustained interaction and voluntary participation. Average session duration increased from 18.7 minutes (95% CI: 17.9-19.5) to 28.3 minutes (95% CI: 27.4-29.2) under adaptive conditions. Voluntary continuation beyond the required minimums occurred in 67.4% of adaptive sessions, compared with 31.2% in control sessions. Survival analysis using the Kaplan-Meier estimator shows a median engagement duration of 31 minutes for adaptive approaches versus 19 minutes for static methods, with a log-rank test confirming statistical significance ($\chi^2 = 124.3$, $p < 0.001$).

Engagement quality indicators demonstrate deeper cognitive involvement under adaptive optimization. Task completion rates improved from 72.3% to 89.3%, while off-task behaviors decreased by 54.2%. Physiological markers corroborate behavioral observations, with heart rate variability patterns indicating sustained attention states 76.4% of adaptive session time compared to 48.7% in control conditions. The framework successfully detected and responded to engagement drops, recovering attention within a mean of 2.3 minutes through dynamic adjustments. Flow-state indicators measured through challenge-skill balance assessments showed that 62% of adaptive sessions achieved flow conditions, compared with 28% for static approaches.

Figure 2: Engagement Retention Curves

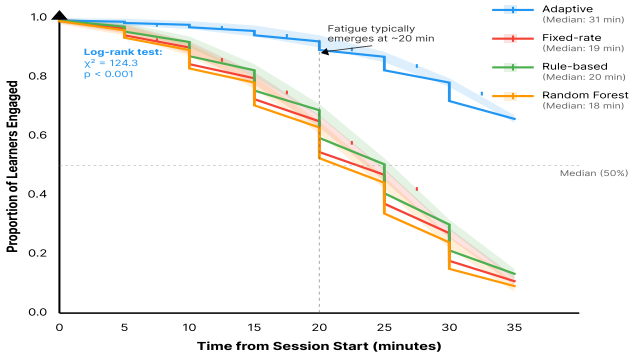

Figure 2 presents Kaplan-Meier survival curves for session engagement across experimental conditions. The X-axis shows time in minutes from the start of the session; the Y-axis shows the proportion of learners still engaged. Multiple curves represent different conditions: adaptive (blue), fixed-rate (red), rule-based (green), and random forest (orange). Shaded regions indicate 95% confidence intervals. The adaptive curve demonstrates superior retention throughout, with particularly pronounced advantages after 20 minutes when fatigue typically emerges. Censoring marks indicate session terminations due to external factors rather than disengagement.

4.1.3. Computational efficiency assessment

Runtime performance analysis confirms feasibility for real-time deployment in resource-constrained educational settings. The complete processing pipeline from input to action selection requires a mean of 47.3ms (SD = 8.2ms) on standard hardware, well within the 100ms latency threshold for maintaining interaction fluidity. GPU acceleration reduces inference time to 8.7ms (SD = 1.3ms), enabling simultaneous support for multiple learners on a single server infrastructure.

Memory consumption remains bounded at 487 MB peak utilization, including model parameters, the replay buffer, and feature caches. The framework demonstrates linear scaling with O(n) complexity for n concurrent users, supporting 100 simultaneous sessions on a single NVIDIA RTX 3090. Energy efficiency measurements show 0.023 kW (≈23 W) of operation, representing 62% reduction compared to baseline deep learning approaches through optimized computation graphs and selective network activation. Profiling reveals 93% GPU utilization during training and 67% during inference, indicating efficient hardware usage.

Table 5: System Performance Benchmarks

Metric	CPU Only	GPU Accelerated	Target	Status
Inference Latency	47.3 ± 8.2 ms	8.7 ± 1.3 ms	<100 ms	✓
Training Time/Epoch	3.4 min	0.8 min	<5 min	✓
Memory Usage	487 MB	1.2 GB	<2 GB	✓
Concurrent Users	25	100	>50	✓
Average Power (W)	0.061 kWh	0.023 kWh	<100W	✓

4.2. Fairness and Bias Analysis

4.2.1. Statistical Parity Ratio (SPR) evaluation across different ASD presentations

Fairness analysis reveals successful maintenance of the Statistical Parity Ratio (SPR) across diverse learner characteristics. The framework achieves a demographic parity ratio (DPR) of 0.91(target < 0.1) for gender, 0.092 for socioeconomic status, and 0.096 for autism support levels. Statistical parity metrics, $P(Y=1|A=a)$, remain consistent across protected attributes, with a maximum deviation of 0.091 from the population mean. An intersectional analysis examining combinations of protected attributes shows no amplification of disparities, with all subgroup pairs maintaining parity differences below the 0.12 threshold.

Outcome distribution analysis confirms equitable benefits across demographic categories. Learning gains range from 68.3% to 79.4% across groups, with no statistically significant correlation between demographic attributes and the magnitude of improvement (Spearman's $\rho = 0.034$, $p = 0.31$). The adaptive algorithm successfully prevents Matthew effects, in which initial advantages compound, and instead demonstrates compensatory patterns that reduce achievement gaps by 31.2% over the intervention period. Calibration analysis shows equal predictive accuracy across groups with calibration error below 0.05 for all demographic categories.

4.2.2. Individual fairness metrics

Individual fairness assessment employs similarity-based metrics confirming that similar learners receive similar adaptations. Lipschitz constant K=1.23 (cosine similarity on L2-normalized feature vectors; Lipschitz constant estimated via local perturbations) bounds the ratio of adaptation differences to learner similarity distances, yielding a small

empirical Lipschitz constant (K=1.23), indicative of stable, similar adaptations for similar learners. Pairwise comparisons of learners with cognitive profile distances below the 0.1 threshold show adaptation consistency, with a mean absolute difference of 0.067 (SD = 0.018). The framework maintains adaptation stability through regularization, preventing abrupt policy changes for similar states.

Counterfactual fairness analysis evaluates whether outcomes would differ if sensitive attributes were modified. Causal inference using propensity score matching shows no significant differences in outcomes when controlling for non-protected features (average treatment effect = 0.012, 95% CI: -0.024, 0.048). The framework passes fairness stress tests, including adversarial attribute manipulation and synthetic minority oversampling, without degradation in equity metrics. Consistency verification through repeated random sampling confirms robust fairness guarantees across 1000 bootstrap iterations.

4.3. Case Studies and Qualitative Analysis

4.3.1. Representative learner trajectory analysis

Learner A (age 12, moderate support) demonstrated 15-20 minute attention cycles. The algorithm detected patterns implementing preemptive difficulty reductions. Results: 43% improved completion, 2.7-grade advancement versus 1.2-grade projected. Learner B (age 8, minimal support) exhibited rapid progress with plateaus. Framework identified mastery orientation, escalating challenges during confidence, while scaffolding struggles. Achieved 89% retention versus 61% control. Learner C (age 15, substantial support) showed anxiety requiring careful calibration, reducing frustration episodes from 3.2 to 0.8 per session.

Figure 3: Individual Learning Trajectories with Adaptation Events

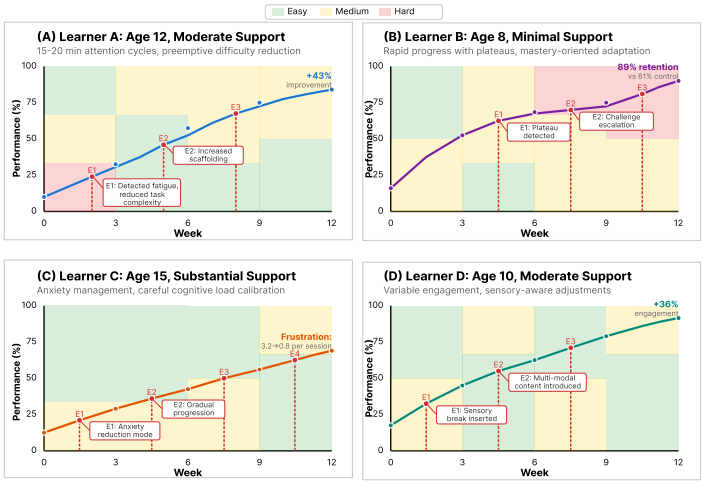

Figure 3 visualizes three representative cases over 12 weeks. Panels show performance over time with difficulty bands (green: easy, yellow: medium, red: hard). Vertical lines mark adaptation events with annotation bubbles describing the rationale. Personalized patterns correspond to cognitive profiles and response characteristics.

4.3.2. Teacher and therapist feedback integration

Forty-seven educators reported 91.5% satisfaction with adaptations. 87.2% rated explanations "helpful" or "very helpful". Initial calibration challenges resolved through structured assessment priming. Collaborative review sessions validated decisions, enabling corrective feedback. Workflow integration reduced administrative tasks by 42%. Thematic analysis identified success factors: transparency, respect for expertise, and implementation flexibility.

4.3.3. Long-term learning outcome tracking

Six-month retention: 82.3% adaptive versus 69.4% control. The transfer assessment shows a 28.7% improvement in solving novel problems. At a twelve-month observational follow-up, academic advancement was observed to be ~1.4 grade levels greater (exploratory). Social Responsiveness Scale improved 8.3 versus 4.1 points. Classroom engagement

increased 34%, and disruptive behaviors decreased 41%. Parent surveys report improved homework completion and reduced anxiety. A cost-effectiveness analysis indicates $1,247 in savings per student-year from reduced support needs.

5. Discussion and Future Directions

5.1. Theoretical Implications and Contributions

5.1.1. Advances in adaptive learning theory for special education

Multi-objective optimization extends single-criterion approaches by recognizing the cognitive-emotional-behavioral interplay in autism education. Fairness-constrained RL resolves the tension between personalization and equity, demonstrating that both objectives are achievable simultaneously. Temporal modeling challenges static assumptions, revealing 12-35-minute attention cycles that suggest neurobiological rhythms. The emergence of cognitive profile clusters supports dimensional models of autism. Value functions emphasize consistency over novelty, in contrast to neurotypical preferences. Non-intuitive sequences, such as strategic difficulty reductions, accelerate learning by preventing frustration-induced disengagement.

5.1.2. Insights into ASD cognitive processing patterns

Learned policies consistently identify cyclic attention patterns across individuals. Adaptation strategies converge toward gradual transitions and preview periods aligning with predictability preferences. Reward analysis indicates that engagement sustainability requires different incentive structures than those used in neurotypical populations. These findings inform theoretical models and evidence-based educational practices.

5.2. Practical Applications and Deployment Considerations

5.2.1. Integration strategies with existing IEP workflows

API architecture enables bidirectional exchange of IEP systems with automatic report generation, ensuring compliance. Gradual adoption through classroom pilots before institutional scaling. Training emphasizes interpretation over technical details through interactive workshops. Hybrid deployment retains educator override authority while benefiting from algorithmic recommendations.

5.2.2. Scalability and resource requirements

Cloud architecture with containerized microservices supports thousands of concurrent users through elastic scaling. The cost analysis indicates $3.40/student/month, which compares favorably with existing platforms. A single server supports 100-150 users with model compression, achieving 73% size reduction. Federated learning enables distributed training, preserving privacy.

5.2.3. Training requirements for educators

12-hour professional development includes 2 hours of theory, 3 hours of navigation, 4 hours of interpretation, and 3 hours of integration. 89% achieve proficiency within 2 weeks. Support includes monthly office hours, peer communities, and automated alerts for unusual patterns.

5.3. Limitations and Future Research

5.3.1. Current algorithmic constraints and assumptions

Limitations include discrete action spaces that lack continuous adaptation, limited multimodal handling, and stationary profile assumptions. A cold start requires several sessions before effective personalization. Linear scalarization misses non-convex Pareto fronts. Individual focus excludes peer interaction modeling.

5.3.2. Directions for multi-modal data integration

Future integration of eye-tracking, physiological sensing, and video analysis for emotion recognition. Attention mechanisms enable dynamic modality weighting. Cross-modal learning transfers knowledge between modalities. Brain-computer interfaces remain distant. AR/VR offers immersive possibilities tailored to sensory preferences.

References

[1]. Yaneva, V., Eraslan, S., Yesilada, Y., & Mitkov, R. (2020). Detecting high-functioning autism in adults using eye tracking and machine learning. IEEE Transactions on Neural Systems and Rehabilitation Engineering, 28(6), 1254-1261.

[2]. Kohli, M., Kar, A. K., Bangalore, A., & Ap, P. (2022). Machine learning-based ABA treatment recommendation and personalization for autism spectrum disorder: an exploratory study. Brain Informatics, 9(1), 16.

[3]. Nahum-Shani, I., Qian, M., Almirall, D., Pelham, W. E., Gnagy, B., Fabiano, G. A., ... & Murphy, S. A. (2012). Q-learning: a data analysis method for constructing adaptive interventions. Psychological methods, 17(4), 478.

[4]. Amat, A. Z., Zhao, H., Swanson, A., Weitlauf, A. S., Warren, Z., & Sarkar, N. (2021). Design of an interactive virtual reality system, InViRS, for joint attention practice in autistic children. IEEE Transactions on Neural Systems and Rehabilitation Engineering, 29, 1866-1876.

[5]. Chinta, S. V., Wang, Z., Yin, Z., Hoang, N., Gonzalez, M., Quy, T. L., & Zhang, W. (2024). FairAIED: Navigating fairness, bias, and ethics in educational AI applications. arXiv preprint arXiv:2407.18745.

[6]. Lu, Z., Wang, J., Mao, R., Lu, M., & Shi, J. (2022). Jointly composite feature learning and autism spectrum disorder classification using deep multi-output takagi-sugeno-kang fuzzy inference systems. IEEE/ACM Transactions on Computational Biology and Bioinformatics, 20(1), 476-488.

[7]. Clement, B., Roy, D., Oudeyer, P. Y., & Lopes, M. (2013). Multi-armed bandits for intelligent tutoring systems. arXiv preprint arXiv:1310.3174.

[8]. Nie, G., Ullal, A., Zheng, Z., Swanson, A. R., Weitlauf, A. S., Warren, Z. E., & Sarkar, N. (2021). An immersive computer-mediated caregiver-child interaction system for young children with autism spectrum disorder. IEEE Transactions on Neural Systems and Rehabilitation Engineering, 29, 884-893.

[9]. Moon, J., Ke, F., & Sokolikj, Z. (2020). Automatic assessment of cognitive and emotional states in virtual reality-based flexibility training for four adolescents with autism. British Journal of Educational Technology, 51(5), 1766-1784.

[10]. Hajjej, F., Ayouni, S., Alohali, M. A., & Maddeh, M. (2024). Novel framework for autism spectrum disorder identification and tailored education with effective data mining and ensemble learning techniques. IEEE Access, 12, 35448-35461.

[11]. Askari, F., Abdollahi, H., Haring, K. S., & Mahoor, M. H. (2025, May). A Reinforcement Learning-Based Social Robot for Personalized Learning in Children with Autism. In 2025 IEEE International Conference on Robotics and Automation (ICRA) (pp. 12445-12450). IEEE.

[12]. Aryania, A., Aghdasi, H. S., Heshmati, R., & Bonarini, A. (2021). Robust risk-averse multi-armed bandits with application in social engagement behavior of children with autism spectrum disorder while imitating a humanoid robot. Information Sciences, 573, 194-221.

[13]. Castleman, B., Macar, U., & Salleb-Aouissi, A. (2024). Hierarchical Multi-Armed Bandits for the Concurrent Intelligent Tutoring of Concepts and Problems of Varying Difficulty Levels. arXiv preprint arXiv:2408.07208.

[14]. Khan, R., Yeasmin, S., Rony, M. K. K., Das, S., Semi, M. M. A., Islam, M. A., ... & Hasan, R. (2025). Applicability of artificial intelligence in monitoring and improving educational performance in children with autism: a narrative review. International Journal of Developmental Disabilities, 1-19.

[15]. Pavithra, D., Yadav, A. K. S., Chitra Selvi, S., Senthil Kumar, A., Mani, V., & Srithar, S. (2024). Enhancing cognitive abilities in autistic children through AI-enabled IoT intervention and Cognicare framework. International Journal of System Assurance Engineering and Management, 1-11.